NUMERICALLY MODELING THE MECHANICAL RESPONSE OF POLYMER BONDED EXPLOSIVES

J.M. Gerken*, J.G. Bennett*, and F.W. Smith†

There has been a significant amount of recent interest concerning the numerical modeling of the mechanical response of Polymer Bonded Explosives (PBX). A part of this effort is an experiment called the Mechanically Coupled Cook Off (MCCO) experiment in which a confined piece of explosive is subjected to a uniform temperature increase. The results provide an excellent opportunity to validate aspects of numerical models for explosives. This paper presents developments in finite element modeling techniques that have made it possible to numerically predict these responses. The constitutive behavior of the explosive is modeled via a newly developed material model called ViscoSCRAM, which captures the rate dependence, damage accumulation and mechanical and chemical heating that is apparent in PBX-9501. The cracking is modeled via a newly developed 2-D discrete crack model that captures macroscopic cracking behavior and the geometry changes that accompany discrete fracture. With the inclusion of these two models in standard finite element modeling techniques, it is shown that the numerical models qualitatively reproduce the experimental results.

INTRODUCTION

High explosives (HE) are used in a variety of applications and unexpected explosions of HE could have significant consequences. Because of this, the response of HE to a variety of dynamic loading conditions which might be encountered in real-world situations is of significant interest and is being studied extensively [1,2,3]. Until recently, the response of these materials in specific practical engineering situations has been predicted based upon the results of extensive experimentation [4,5]. However, recent advances in numerical modeling techniques have shown promise for predicting the response of HE in such situations.

The work presented in this paper is an effort to validate some of these techniques by numerically modeling an experiment known as the Mechanically Coupled Cook Off (MCCO) experiment [6]. In this experiment the "cook-off" of the explosive PBX 9501 is reproduced by confining a small circular slab of the High Explosives (HE) material in a circular metal ring and then subjecting the assembly to a uniform temperature increase. As the temperature increases, the HE undergoes a transition from a response that is primarily

*Los Alamos National Laboratory, ESA-EA MS P946, Los Alamos, New Mexico 87545

†Colorado State University, Department of Mechanical Engineering, Fort Collins, Colorado 80525

thermo-mechanical to a response that is characterized by coupled mechanical, thermal and chemical reaction behaviors occurring under highly dynamic conditions.

The numerical modeling of such an experiment is a difficult task. To predict the behavior observed in these experiments, many different phenomena must be incorporated into the numerical model. Thermal straining has been incorporated into the model to reproduce the stress field and the deformation, which occur due to the thermal expansion mismatch between the metal and the HE. The magnitude of the stress field in the metal confinement becomes large enough that it must be modeled as an elastic-plastic material. A new visco-elastic damage model, called ViscoSCRAM, has been developed to model the mechanical response of PBX 9501 [7]. A new method for modeling discrete cracking in a finite element mesh is used to model the macroscopic crack propagation in the HE [8]. The remainder of this paper will present a brief description of the experiment and how these numerical techniques are used to model the experiment.

MCCO EXPERIMENT

A cartoon of the MCCO experiment is shown in Fig. 1. A small flat cylinder of PBX 9501 is confined in a metal ring of copper or mild steel of various thickness (6.35 mm, 3.175 mm, and 1.588 mm have been used). The HE and ring assembly is confined between a window at the top and a solid metal surface at the bottom. The HE specimen has an outer diameter of 25 mm and an inner diameter of 3.175 mm. To simulate the cook-off event, the HE is heated uniformly from both the top and bottom. For the experiments simulated here, the sample is heated to a temperature below the auto-ignition temperature, at which point the decomposition gasses present in the inner hole are ignited by an electrically heated NiCr wire.

Figure 1. Setup of MCCO experiment.

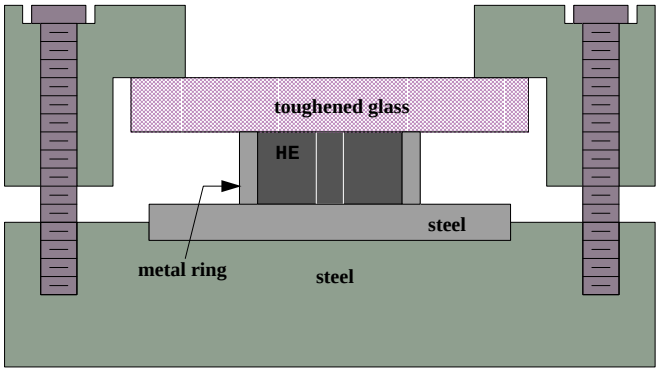

Experimental observations are made in several ways including the use of a camera that photographs the reacting HE at intervals of 3 to 5 μsec through the top window. The sequence of photographs presented in Fig. 2 shows the behavior of HE in a MCCO

experiment after the onset of the chemical reaction. The specimen shown in the figure was confined in a 3.175mm thick copper ring, heated to 190°C in about 1 hour, and ignited with a NiCr wire. The photographs show narrow regions of lumination propagating from the inner surface outward toward the confinement ring. This lumination is thought to be caused by the ignition of fresh HE surface behind discrete cracks as they propagate radially out from the inner surface of the specimen [6]. The photographs show that early in the process, at about 0 to 5 μsec after the start of observation, there appear to be three narrow cracks starting to propagate outward. The largest of the three cracks then branches into two different cracks at about 10 μsec, still propagating in a somewhat radial direction. As time progresses, much of the HE has started to chemically react and the lumination overwhelms the details of discrete cracks and branching phenomena observed earlier. In this experimental configuration, it is typically observed that 3 to 4 radial cracks propagate radially after ignition and that such cracks may subsequently bifurcate. Other configurations of the MCCO experiment produce results that are a bit different from those discussed here. For the purpose of validating the numerical models, this particular configuration is the only one that has been numerically modeled to date.

Figure 2. Optical photographs of MCCO experiment.

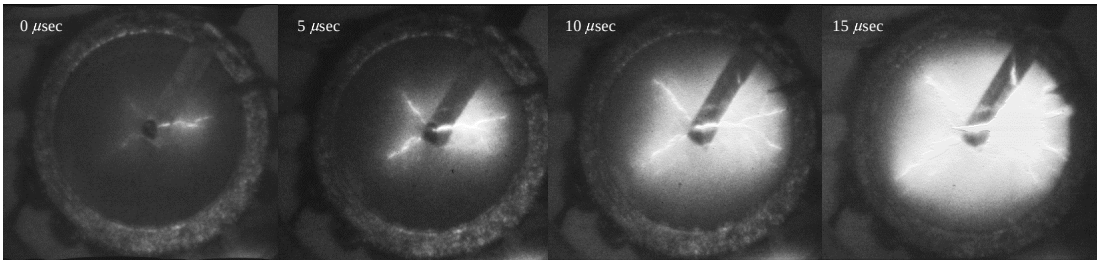

NUMERICAL MODEL

Because the time scale of the experiment ranges from approximately 10^{2} to 10^{-6} seconds and the complex nature of the experiment requires a non-linear model, the implicit finite element method was chosen as the framework for the current work. The upper and lower constraints on the HE and confinement ring do not allow significant straining in the axial direction, therefore, a two-dimensional plane strain model is sufficient.

Within the two-dimensional non-linear implicit finite element framework many phenomena must be incorporated to accurately model the MCCO. As the sample assembly is heated, the free thermal expansion of the HE would be greater than that of the metal confinement. In the constrained state, this expansion mismatch causes a stress state in the metal that exceeds the material's yield strength. Also a gas pressure pulse due to the ignition of HE decomposition gases is applied to the exposed surface of the HE. This large pressure pulse causes tensile hoop strain in the HE near the inner surface, which, in turn,

causes discrete cracks to form that propagate radially outward. As these discrete cracks open up and propagate, the gas pressure also acts on the crack faces and applies an additional crack opening load. The entire process is extremely dependent on the mechanical and thermal nature of the PBX 9501, which is a history and rate-dependent nonlinear material that has complex constitutive behavior.

Thermal expansion, metal plasticity and mechanical loading can be incorporated into an implicit finite element method with relative ease therefore their implementation is not discussed here. Discrete cracking and the material model of PBX 9501 are relatively new models so discussion of some of the details of these two models is included in the following.

Discrete Cracking

A brief description of the model for discrete cracking developed by Gerken [8], with some modification to allow for material non-linearity, is presented here. The model allows for discrete crack propagation along any pre-existing finite element edges, thereby allowing discrete crack propagation along arbitrary paths without the need for *a priori* assessment of the crack paths.

For the discrete fracture method, a single finite element consists of four unique nodes (as opposed to shared nodes in standard finite elements) with small cracks located at each interface with an adjacent finite element. Shown in the cartoon in Fig. 3, each element is defined by unique nodes with displacement continuity maintained for collocated nodes. This definition allows for the elements to maintain their original nodal connectivity as discrete cracks propagate along element interfaces. Also shown in the cartoon, is the conceptual representation of a single element. Because a four-sided element can be adjacent to as many as four other elements, each element is represented as a standard finite element with a single crack on its edge. If there is more than one crack on the element edge, the additional cracks are treated as independent cracks and are additive to the original definition.

Figure 3. Graphical representation of the finite elements used for discrete fracture.

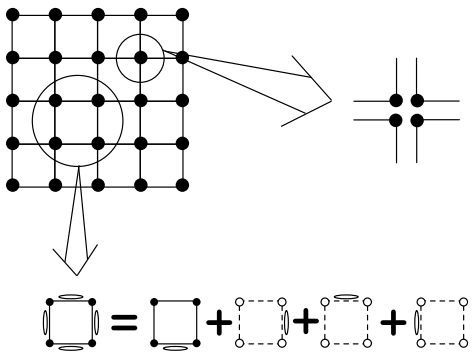

A representation of the field equations can be developed from the Hu-Washizu Energy Principle [9]. This principle is the foundation of the finite element equations used in the discrete fracture model and is given here in matrix form as

$$\Pi_{HW}(\mathbf{u},\boldsymbol{\sigma},\boldsymbol{\varepsilon}) = \int_{\Omega}\left[\frac{1}{2}\boldsymbol{\varepsilon}^{\mathrm{T}}\mathbf{D}\boldsymbol{\varepsilon} - \boldsymbol{\varepsilon}^{\mathrm{T}}\mathbf{D}\boldsymbol{\varepsilon}_0 + \boldsymbol{\varepsilon}^{\mathrm{T}}\boldsymbol{\sigma}_0 + \boldsymbol{\sigma}^{\mathrm{T}}(\mathbf{L}\mathbf{u} - \boldsymbol{\varepsilon})\right]\mathrm{d}\Omega - \Pi_{EXT} \qquad (1)$$

where the independent variables **u**, σ, and ε are displacement, stress and strain fields respectively, Ω is the element volume (or area for a two-dimensional element), **D** is the elastic moduli coefficients matrix, ε_0 and σ_0 are the initial strain and stress tensors respectively, Π_{EXT} is the external work, and **L** is the strain displacement operator. To incorporate the effects of the edge cracks into the formulation, the external work term, Π_{EXT}, is assumed to include work due to an external strain field applied to the element. This external strain field is the strain field in the element due to a small crack on its surface. Shown in Fig. 4, this strain field is determined by analyzing a small crack in an infinite linear elastic plate subject to the far-field stresses shown. The strain field in the plate due to the crack can be obtained analytically and included in the external work term, Π_{EXT}.

Figure 4. Strain field from a small crack applied to the finite element as external work.

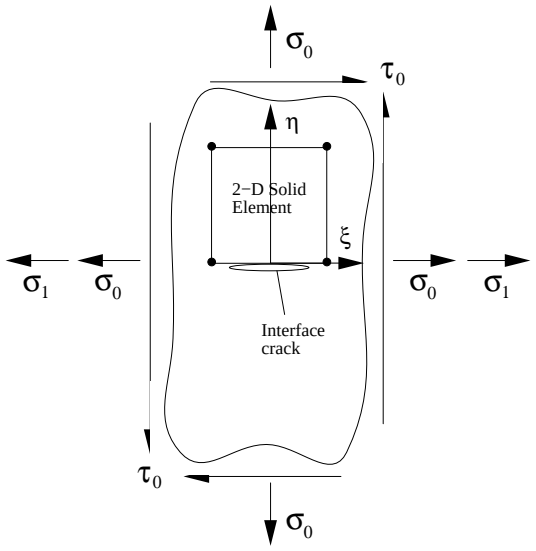

It can be shown by taking the first variation of Π_{HW} and making appropriate approximations for **u**, σ, and ε, that the following matrix equation results

$$\mathbf{K}\mathbf{d} = \mathbf{f} + \mathbf{F}_0 + \sum_{i=1}^{n}\mathbf{Q}_i\ , \qquad (2)$$

where **K** is the stiffness matrix, **d** is the vector of nodal displacements, **f** and $\mathbf{F}_0$ are the body force and initial condition load vectors and $\mathbf{Q}_i$ is the additional load vector due to a single small crack on the element edge, with *n* being the number of edge cracks. If there are no interface cracks, $\mathbf{Q}_i \equiv$**[0]** and Eqn. 2 simplifies to the standard two-dimensional finite element equations derived from the Hu-Washizu Energy Principle. It should be noted that in Gerken's work [8], the analysis is linear and the initial stress and strain are assumed to be zero. For use in the numerical model presented here, the initial condition load vector, $\mathbf{F}_0$, has been taken into account, where ε_0 and σ_0 are relative to the current solution increment, not the initial conditions at the start of the solution.

By defining each element with unique node numbers, the elements can separate from adjacent elements and still maintain their original nodal connectivity. This separation simulates discrete crack growth. To accurately model the fracture process, appropriate failure criteria for interface failure must be defined. The small crack at the interface can be approximated to behave like a small crack in an infinite elastic plate. The far field stresses acting on the infinite plate are assumed to be the average stresses from the edges of the two adjacent elements so that the local strain energy release rate can be determined from the following equations:

$$K_I = \bar{\sigma}_I \sqrt{\pi \cdot a}\ ;\ K_{II} = \bar{\tau}_{II} \sqrt{\pi \cdot a}\ ,$$

$$G = \frac{K_I^2 + K_{II}^2}{E}, \qquad \text{(3 a, b, c)}$$

where the overbar denotes averaged quantities, σ_I and τ_{II} are tensile and shear stresses, and *a* is the interface crack half-length, and *E* is the elastic modulus of the material. The growth of the small crack is assumed to be governed by the materials strain energy release rate which can be approximated with

$$G = \beta(\Delta a)^{\gamma} + \lambda\ , \qquad (4)$$

where *G* is the strain energy release rate, *a* is the crack half width, and β, γ, and λ are curve fitting parameters. Equation 4 can then be rearranged to give the change in crack length given the strain energy release rate and the other parameters in the form

$$\Delta a = \left(\frac{G - \lambda}{\beta} \right)^{\frac{1}{\gamma}}. \qquad (5)$$

Hence, given the stresses from the two adjacent elements, the local strain energy release rate is determined. Then, at the end of a time step in the finite element simulation, the change in crack length of the interface crack is determined. If the interface crack grows to be wider than the length of the element edge, the interface fails and is allowed to separate.

ViscoSCRAM

Another significant part of the numerical model of the MCCO experiment is the constitutive behavior of PBX 9501. The ViscoSCRAM material model has been developed to model the following observed characteristics of PBX 9501; 1) irreversible material damage, 2) visco elastic material response, 3) adiabatic mechanical heating, 4) chemical heating, 5) non-shock ignition. This material model has been developed by Bennett et al. [10] for explicit finite element applications and by Hackett and Bennett [7] for implicit finite element implementations. The underlying principles of both methods are identical, however, the implicit model is of interest here, therefore, a brief description of the model developed by Hackett and Bennett is presented.

The mechanical response is accomplished by coupling an isotropic material damage model with an isotropic, generalized Maxwell visco elastic model. Assuming the mean components of the material behavior are linear elastic, a three dimensional generalization shows that the total deviatoric strain rate can be represented as follows

$$\dot{e}_{ij} = \dot{e}_{ij}^{ve} + \dot{e}_{ij}^{dm}, \tag{6}$$

where the dot indicates a rate, e_{ij} is the deviatoric strain tensor, and the superscript *ve* and *dm* denote the visco elastic and damage portions respectively. These strain rates are given by

$$\dot{e}_{ij}^{ve} = \frac{1}{2\mathrm{G}}\left(\dot{s}_{ij} + \sum_n \frac{s_{ij}^{(n)}}{\tau^{(n)}} \right),$$

$$\dot{e}_{ij}^{dm} = \frac{1}{2\mathrm{G}}\left(3\mathrm{C}^2\dot{\mathrm{C}}s_{ij} + \mathrm{C}^3\dot{s}_{ij}\right), \tag{7a, b}$$

where n represents the number of dashpots, G is the shear modulus (summation of shear moduli in the Maxwell model), s_{ij} is the deviatoric stress tensor, τ is the relaxation time, and C is an evolving damage variable. Development of the above governing equations shows the deviatoric stress-strain relationship for the numerical model is as follows

$$\dot{s}_{ij} = \frac{2\mathrm{G}\dot{e}_{ij} - \sum_n \frac{s_{ij}^{(n)}}{\tau^{(n)}} - 3\mathrm{C}^2\dot{\mathrm{C}}s_{ij}}{1+\mathrm{C}^3}. \tag{8}$$

After selection of an appropriate evolution law for the damage parameter, C, Eqn. (8) defines the mechanical behavior of the numerical model.

Internal thermal generation includes mechanical work and chemical decomposition due to both temperature and loading effects. Taking into account the mechanical and chemical

heating terms and neglecting conduction, an energy balance on a differential volume of the material gives the rate of change of the temperature with respect to time as

$$\frac{\partial T}{\partial t} = -\gamma T \dot{\varepsilon}_{kk} + \frac{\Im}{\rho C_v}\left[\left(\rho T \dot{s}\right)_{ve} + \left(\rho T \dot{s}\right)_{dm}\right] + P_{he}\dot{q}_{ch} \tag{9}$$

where the right hand side terms above represent the following thermal effects

- $\gamma T \dot{\varepsilon}_{kk}$ = adiabatic compression heating rate
- $\frac{\Im}{\rho C_v}\left[\left(\rho T \dot{s}\right)_{ve} + \left(\rho T \dot{s}\right)_{dm}\right]$ = inelastic work rates due to viscous effects and cracking damage
- $P_{he}\dot{q}_{ch}$ = bulk chemical heating

where the non-material parameters are

$$\dot{\varepsilon}_{kk} = \dot{\varepsilon}_{11} + \dot{\varepsilon}_{22} + \dot{\varepsilon}_{33},$$

$$\left(\rho T \dot{s}\right)_{ve} = \sum_n s_{ij}^{(n)} \dot{e}_{ij}^{ve},$$

$$\left(\rho T \dot{s}\right)_{dm} = s_{ij} \dot{e}_{ij}^{dm}, \tag{10a, b, c}$$

and the chemical heat generation, $\dot{q}_{ch}$, is obtained by assuming a heat generation term at sliding crack faces due to Arrhenius first order chemical kinetics then using a weighted residual method to solve the one dimensional Frank-Kamenetski equations [11] that govern heat transfer near a crack face.

MCCO MODEL

Shown in Fig. 5, a plane strain model of the copper confinement ring and the PBX 9501 has been developed for analysis in ABAQUS/Standard (ABAQUS). The PBX 9501 has an inner diameter of 3.175 mm and an outer diameter of 25.4 mm. The inner diameter of the copper ring matches the outer dimension of the HE with the thickness being 3.175 mm giving an outer diameter of the confinement ring of 31.75 mm. The PBX 9501 consists of 1200 discrete fracture elements. The radial dimension of the HE elements varies from 0.24 mm at the inner row of elements to 0.87 mm for the outer row of elements. The tangential dimension of the HE elements varies from 0.17 mm for the inner row to 1.33 mm for the outer row. Because it has not been observed in the experiments, it is assumed that the copper confinement ring will not crack, therefore, standard plane strain elements are used to model the confinement ring. The interface between the copper and the HE is modeled as

an infinite strength bond so that the interface is allowed to deform, but no relative motion between the HE and the copper is allowed.

Figure 5. Finite element mesh of the HE and copper ring for the MCCO experiment.

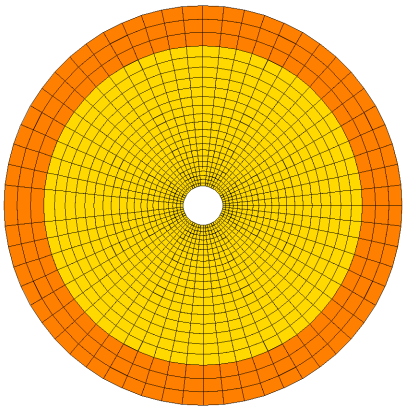

An isotropic elastic plastic material model was used to model the response of the copper. The material has an elastic modulus of 117 x 10^9 Pa and a Poisson's ratio of 0.33. The stress vs. plastic strain was obtained using a power law model with a yield stress of 65 MPa, a strain hardening exponent of 0.2 and a yield stress coefficient of 292 MPa. The coefficient of thermal expansion of copper is a constant 16.56 x 10^{-6} /°C and the density is 8.9 x 10^3 kg/m^3.

The ViscoSCRAM constitutive model described earlier was used to represent the behavior of the PBX 9501. The constant coefficient of thermal expansion for PBX 9501 is 55 x 10^{-6} /°C and the density is 1.849 x 10^3 kg/m^3. For the conditions of the experiment it is likely that the material properties are not constant. However, for the present, they are taken to be constant throughout the entire temperature range.

For the discrete fracture model, each element interface in the HE has been seeded with a small crack. The size of these interface cracks is randomly distributed throughout the mesh according to an approximately flat distribution such that the largest crack is approximately 90% of the smallest element width and the smallest crack is approximately 10% of the smallest element width. This type of definition allows for the failure conditions for fracture to be different for each interface. Also, by choosing several different sets of samples to represent the same flat distribution and mean crack size, the relationship between the general features of the results and any particular set of interface cracks can be ascertained.

The fracture properties of PBX 9501 have been estimated based on the limited information that is available for HE. The fracture parameters from Eqn. (4) used in the

present simulation to model the fracture behavior of the HE are $\beta = 2.0$, $\gamma = 0.1$, and $\lambda = 0.0$.

To reproduce the conditions of the experiment, the analysis simulated heating from room temperature at a rate of 0.6 °C/sec for 200 seconds. During this heat-up phase, only the mechanical response of the HE is enabled. The large time scale of this phase would allow ample time for the entire apparatus to come to thermal equilibrium and the chemical and mechanical heating modeled in ViscoSCRAM can be neglected. After this initial phase, a pressure pulse of 5 MPa/μsec was applied to the inner surface of the HE to simulate the rapid pressurization caused by the ignited decomposition gases present in the cavity. This internal pressure causes a tangential stress to develop in the HE and, as a result, cracks begin to open. As these cracks open, the pressure applied to the inner surface is also instantly applied to the crack faces.

RESULTS

The numerical model essentially consists of two different regimes; the heat-up regime and the reactive regime. The heat-up phase is a relatively long-time event that is characterized by slow material straining with the build up of stresses. The reactive phase, initiated after the heat-up phase, consists of very short-time events including discrete fracture, mechanical and thermal heating, and further, high rate, deformation.

During the heat-up phase of the experiment, both the confinement ring and the HE thermally expand. Because the coefficient of thermal expansion of HE is greater than that of copper, the copper ring serves as a restraint to the expansion of the HE. Shown in Fig. 6 are the effective stress contours in the model after a heat up of 120 K. The high effective stresses on the inner surface of the HE in Fig. 6a are due primarily to high compressive tangential stresses. Because this phase of the experiment is a slow process, the rate of deformation is slow so that the viscous part of the ViscoSCRAM material model does not significantly affect the stress strain behavior of the HE. The high stresses in the confinement ring in Fig. 6b are due primarily to high tensile tangential stress. These stresses are high enough that the entire ring has exceeded the elastic limit before the end of the heat-up phase.

After the heat-up, a pressure pulse of 5MPa/μsec is applied to the inside of the HE. The compressive stresses in the inner row of elements are never overcome, likely due to damage and flow of these elements. As the pressure is increased, the stresses in the second (from the inner surface) row of elements transitions to tension. This tension creates strain energy that causes the interface cracks to eventually fail, starting with the largest interface crack. As cracks fail and open up, tensile stresses in the vicinity of the crack are relieved, thereby reducing the strain energy in nearby elements. In addition to relieving nearby tensile stresses, these discrete cracks also create large stress concentrations in front of the crack, encouraging further growth in the radial direction. Crack growth is further

encouraged by the application of the internal pressure to the crack faces, which increases the tensile stress acting on the crack. Shown in Fig. 7 is a graphic of a typical simulation in which many small discrete fractures appear early in the simulation.

Figure 6. Effective stress contours for the model after the heat up phase.

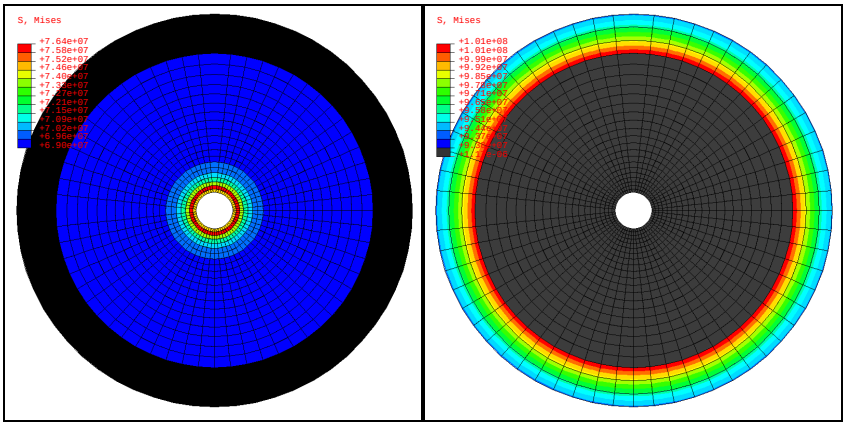

As simulation time progresses, some of these small cracks will continue to propagate radially outward and some will arrest. The cracks that propagate to become large cracks are thought to be the cracks that would be visible in the experimental photographs. In all of the simulations run to date, 3 – 5 large cracks appear and propagate from near the inner surface to near the copper confinement ring with several smaller arrested cracks. Shown in Fig. 8 is a plot of the final deformed shape of a typical simulation in which 3 large cracks appear. The time in the simulation is 28.8 μsec after the heat-up, corresponding to an internal pressure of 144 MPa. This time corresponds roughly to the "observation time" reported for the MCCO in which luminescence typically reaches the confinement ring at about 10 to 20 μsec after the start of observation

Figure 7. Many small cracks appear early in the simulation. 10x displacement.

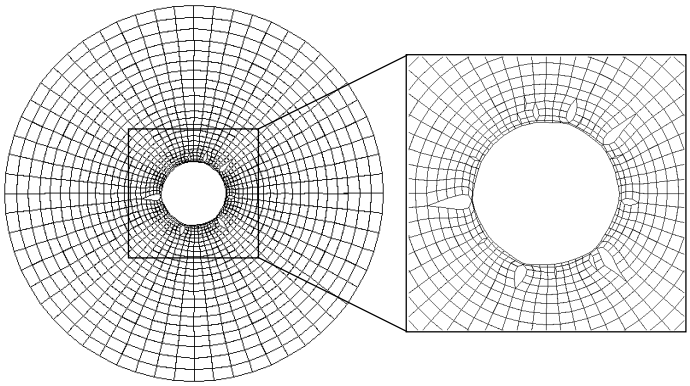

Figure 8. Final deformed shape of an MCCO simulation.

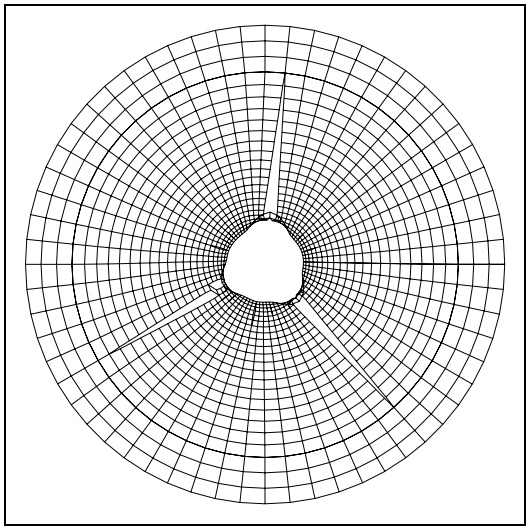

The simulation also provides some insight into processes that are not directly observed by the techniques used in the experiment. It is known that PBX 9501 undergoes decomposition and a temperature rise due to sudden pressure application such as in the experiment [12]. This can be seen in the numerical model as a significant temperature increase in the HE near the inner surface accompanied by a small increase in temperature relative to the surrounding material near the discrete crack faces. Shown in Fig. 9a is a contour plot of the temperature in the HE at the end of a simulation. It shows an increase in temperature from 413 K at the end of heat up to 450 K at locations on the inner surface. It can also be seen that the HE in the region of the large discrete cracks has increased in temperature relative to the surrounding HE. This heating is due to both mechanical work and chemical decomposition.

Shown in Fig. 9b, the simulation predicts an even more pronounced increase in the damage variable in these areas. The damage variable, which has an initial value of 3×10^{-5}, increases to a value of 3×10^{-3} at locations near the interior and has a much more distinct increase, compared to the temperature rise, over the surrounding HE in the area of the discrete cracks.

Numerous simulations have been conducted and they are found to be quite reproducible in terms of the general behavior. Shown in Fig. 10 are four different simulations. Each model is the same except that different sets of random crack sizes, with the same distribution and mean size, have been used to seed the element interfaces. The models show that 3 to 5 large cracks appear and propagate out toward the copper ring. In addition, the total simulation time is similar in all cases with the times relative to the end of the heat-up phase being (from right to left): 27.4 μsec, 26.9 μsec, 29.0 μsec, and 28.8 μsec.

Figure 9. The a) temperature distribution and b) damage in HE at end of simulation shows an increase in both near the inner surface and the large discrete cracks.

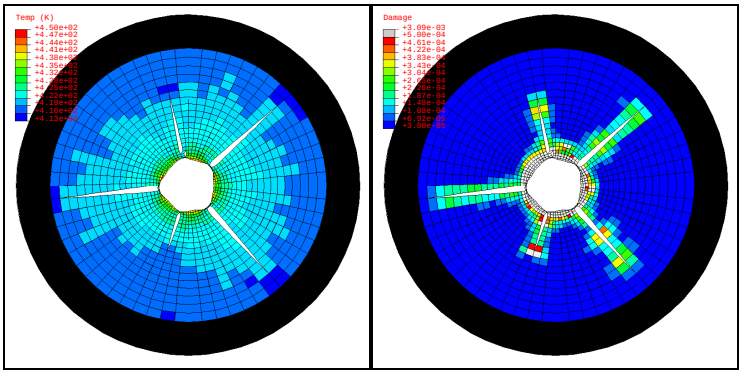

Figure 10. Several simulations show the appearance of 3 to 5 large cracks.

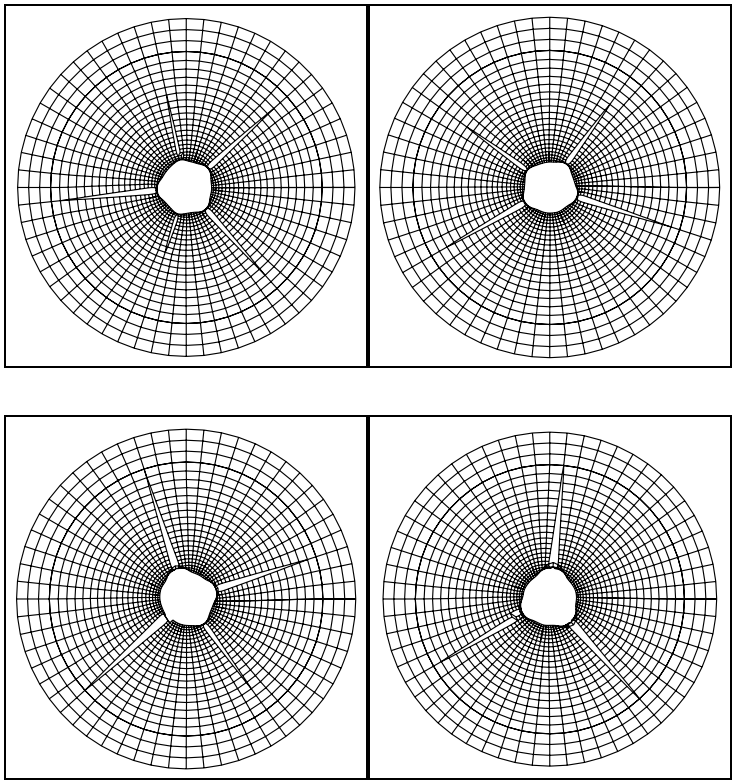

SUMMARY AND CONCLUSION

A finite element model of the Mechanically Coupled Cook Off experiment conducted on PBX 9501 has been developed to help validate some of the HE modeling techniques. Photographs from the experiment show the formation of 3 to 5 large discrete cracks that propagate from the inner surface radially outward toward the confinement ring. The finite element model developed to simulate the experiments includes the behaviors thought to be essential to modeling the observed behavior. Two key components of the numerical model are the ViscoSCRAM material model for PBX 9501 which model both the thermal and mechanical response of the HE and a discrete fracture model which models macroscopic fracture based upon standard fracture criteria. Much is still not known about the behavior of PBX 9501 and many assumptions had to be made and material information had to be surmised from limited data. In spite of these known shortcomings, the incorporation of these models with other standard finite element modeling techniques has produced a model of the MCCO that reasonably well reproduces the photographic observations of the experiment.

REFERENCES

1. McGuire, R.R., and Tarver, C.M., (1981) "Chemical Decomposition Models for the Thermal Explosion of Confined HMX, TATB, RDX, and TNT Explosives", Proceedings, 7th International Symposium on Detonation, Naval Surface Weapons Center, White Oak, Maryland, pp. 56-64.

2. Dienes, J.K., (1984), "A Unified Theory of Flow, Hot-spots, and Fragmentation with an Application to Explosive Sensitivity", High Pressure Shock Compression of Solids II: Dynamic Fracture and Fragmentation, L. Davison et al, eds., Springer, New York, pp. 366-398.

3. Field, J.E., Bourne, N.K., Palmer, S.J.P., and Walley, S.M., (1992), "Hot-Spot ignition Mechanisms for Explosives and Propellants", Philosophical Transactions of the Royal Society of London, A, Vol. 339, pp. 269-83.

4. Howe, P.M., Gibbons, G., Jr., and Webber, P.E., (1985), "An Experimental Investigation of the Role of Shear in Initiation of Detonation by Impact", Proceedings, 8th International Symposium on Detonation, Naval Surface Weapons Center, White Oak, Maryland, pp. 294-306.

5. Gray, G.T., Idar, D.J., Blumenthal, W.R., Cady, C.M., and Peterson, P.D., (1998), "High and Low Strain Rate Compression Properties of Several Energetic Material Composites as a Function of Strain Rate and Temperature", To appear: Proceedings,

11th International Symposium on Detonation, Office of Naval Research, Washington, D.C.

6. Dickson, P.M., Asay, B.W., Henson, B.F., and Fugard, C.S., (1998), "Observation of the Behavior of Confined PBX 9501 following a Simulated Cookoff Ignition", To appear: Proceedings, 11th International Symposium on Detonation, Office of Naval Research, Washington, D.C.

7. Hackett, R.M., and Bennett, J.G. (1999) "An Implicit Finite Element Material Model for Energetic Particulate Composite Materials", Technical Report, LA-UR-99-3139, Los Alamos National Laboratory, Los Alamos, New Mexico.

8. Gerken, J.M., (1998) "An Implicit Finite Element Method for Discrete Dynamic Fracture", MS thesis, Colorado State University, Fort Collins, Colorado.

9. Hu, H.C., (1955), "On Some Variational Principles in the Theory of Elasticity and the Theory of Plasticity", Scientia Sinca, Vol. 4, pp. 33- 54.

10. Bennett, J.G., Haberman, K.S., Johnson, J.N., Asay, B.W., and Henson, B.F., (1998) "A Constitutive Model for the Non-Shock Ignition and Mechanical Response of High Explosives", Journal of the Mechanics and Physics of Solids, Vol. 46, pp. 2303-22.

11. Frank-Kamenetski, A.A., (1942), "On the Mathematical Theory of Thermal Explosions", Acta Physicochimica URSS, Vol. XVI, pp. 357-61.

12. Asay, B.W., Funk, D.J., Henson, B.F., and Laabs, G.W., (1997), "Speckle Photography During Dynamic Impact of an Energetic Material Using Laser Induced Fluorescence", Journal of Applied Physics, Vol. 82, pp 1093-99.